Ecological impact evaluation of urban heat island in Dhaka city; a spatio-temporal approach

Kazi Jihadur Rashid
University of Chittagong Faculty of Biological Science
Sumaia Islam
University of Chittagong
Mohammad Atiqur Rahman (mmd.atiqur.rahman@gmail.com)
University of Chittagong Faculty of Biological Science https://orcid.org/0000-0002-7198-4399

Research Article

Keywords: Dhaka city, Ecological Evaluation Index, LST Trajectory, UHI, UTFVI

Posted Date: August 31st, 2021

DOI: https://doi.org/10.21203/rs.3.rs-307151/v1

Ecological impact evaluation of urban heat island in Dhaka city: A spatio-temporal approach

Abstract

Urban heat island (UHI) is one of the major causes for deteriorating ecology of the rapidly expanding Dhaka city in the changing climatic conditions. Although researchers have identified, characterized and modeled UHI in the study area, the ecological evaluation of UHI effect has not yet been focused. This study uses land surface normalization techniques such as urban thermal field variance (UTFVI) to quantify the impact of UHI and also identifies vulnerable UHI areas compared to land cover types. Landsat imageries from 1990 to 2020 were used at decadal intervals. Results of the study primarily show that intensified UHI areas have increased spatially from 33.1% to 40.9% in response to urban growth throughout the period of 1990 to 2020. Extreme surface temperature values above 31°C have also been shown in open soils in under-construction sites for future developmental purposes. UTFVI is categorized into six categories representing UHI intensity in relation to ecological conditions. Finally, comparative analysis between land use/land cover (LULC) with UTFVI shows that the ecological conditions deteriorate as the intensity of UHI increases in the area. The developed areas facing ecological threat have increased from 9.3% to 19.8% throughout the period. Effective mitigating measures such as increasing green surfaces and planned urbanization practices are crucial in this regard. This study would help policymakers to concentrate on controlling thermal exposure and on preserving sustainable urban life.

Keywords Dhaka city; Ecological Evaluation Index; LST Trajectory; UHI; UTFVI

1 Introduction

Urbanization causes radiation balance alteration that triggers variations in reflective power (Shahmohamadi et al. 2011). The resultant effect makes urban areas warmer than their surrounding countryside. This phenomenon of fluctuating temperatures is known as the Urban Heat Island (UHI) (Oke 1982; Toy and Yilmaz 2010; Stewart and Oke 2012). Notwithstanding the sizes, each urban structure can generate UHI of 0.4 to 11°C hotter than the adjacent suburban areas (Oke 1973; Tzavali 2015). The development of UHI is

fueled by the dynamic interaction of various factors. These factors can generally be asserted as anthropogenic heat, impermeable surfaces, and geometry of urban structures (Ryu and Baik 2012; Li et al. 2020). Recent decades have seen threatening impacts of UHI on the human environment (Watkins et al. 2007; Yow 2007; Ward et al. 2016). Yow (2007) discussed local to global impacts of UHI including human health and comfort, energy consumption, alterations in ecosystems, and climate. For instance, urban warming with changing climate effects on fish communities as well as trophic dynamics of water bodies results in degrading ecological status of the ecosystem (Jeppesen et al. 2010, Pörtner and Peck 2010).

Urban regions that facilitate human society to develop seamlessly but also jeopardize the quality of the environment and ecosystem as well. Degradation of the environmental quality increases various diseases and mortality as well as hampers urban productivity (Arnfield 2003; Grimm et al. 2008; Zhou et al. 2014; Zhou et al. 2016). Therefore, contemporary urban researchers are focusing on alleviating and reducing UHI (Li et al. 2014; O'Malley et al. 2015; He et al. 2019).

In recent times, the UHI effect can be measured by several methods. Among them, surface UHI assessment by using satellite data is a significant and most recommended method (Voogt and Oke 2003). The surface temperature that emits from land and detects by satellite can play a key role in the age of UHI as a crucial variable (Zhou et al. 2019) in terms of surface radiation and energy transactions. It regulates the circulation of warm air between the surface and the atmosphere. Until now Land Surface Temperature (LST) has been calculated by several algorithms (e.g. Planck Function, Single Channel Algorithm) which are developed in recent times (Li et al. 2013; Avdan & Jovanovska 2016; Ndossi & Avdan 2016; Sahana et al. 2016) . Ndossi & Avdan (2016) compared different algorithms for LST derivation and found that Planck Function produces the best outcomes on both Landsat 05 and Landsat 08. LST normalization indices such as urban thermal field variance (UTFVI) help to better evaluate urban thermal intensities and ecological health (Guha et al. 2018). For maintaining the environmental balance within a city, determining the level of ecological comfort is an important task.

Dhaka is the most populated city in Bangladesh experiencing the fastest urbanization within the world unlike other less developed and developing countries (Seto et al. 2011).

Several attempts have been made to investigate UHI in the city using air temperature, surface temperature from satellite sensor, numerical modeling (Ahmed et al. 2013; Das & Karmakar 2015; Tashnim & Anwar 2016). Das & Karmakar (2015) analyzed the annual temperature data from 1961 to 2000 and also studied the Weather Research and Forecasting (WRF) model, which showed a growing trend of temperature in the city compared to the surrounding districts and found that it was mostly warm during the night and afternoon hours. Kakon & Nobuo (2009) investigated the effect of sky view factor on seasonal solar radiation in the study area. Previous studies on UHI in the study area were mainly focused on UHI intensity, factors, and the correlation of different land cover types with LST (Raja 2012; Dewan & Corner 2014; Mia et al. 2017; Trotter et al. 2017; Rahman et al. 2020). However, much of the research evaluating the impact of UHI up to now in the city has been descriptive and no prior studies have been undertaken to assess the impact of UHI quantitatively.

To address the research gap mentioned above, this study focuses mainly on the spatial-temporal assessment of the impact of UHI on the urban ecosystem over the study area using Landsat images through the period from 1990 to 2020. First, this study analyzes the spatial-temporal variations of LST. Secondly, the study explores the surface cover scenarios and the UHI affected area. Finally, quantitatively evaluates the ecological impact of UHI using the UTFVI.

2 Materials and methods

2.1 Study area

The study area, Dhaka is shown in Fig. 1. It is positioned in central Bangladesh at 23°42′N and 90°22′E. The city has a population of 21,005,860 (2020) approximately with a total area of 306 km2 . The city is located on the lower range of the Ganges Delta which is flat and close to sea level and the land is characterized by tropical vegetation and moist soils under the Köppen climate classification. Dhaka experiences a mean annual rainfall of 2,084.7 millimeters and an average annual temperature of 25.9°C varying between 18.6°C in January and 29 °C in June which resembles a tropical savanna climate (Choudhury 2016).

2.2 Data

Landsat TM (1990, 2000, and 2010) and Landsat OLI/TIRS (2020) were downloaded from the official website of the US Geological Survey (USGS). Spatial resolution of Landsat is 30 meter and images for the study area fall inside the scene of path 137 and row 44. Cloud free images of winter were collected to have similar weather conditions and phenological characteristics. Table 1 illustrates collected data in detail.

2.3 Methodology

All the following procedures were carried out using QGIS software and R programming. Image correction and sampling for LULC were done in QGIS platform. Image classification, LST calculation, and visualization were performed in Rstudio with the help of raster, rgdal, caret packages.

2.3.1 Data processing

Prior to analysis of Landsat imageries, radiometric calibration and atmospheric correction are necessary. All the collected raw bands were converted into top of atmosphere (TOA) reflectance and radiance from digital numbers (DN) to represent physical properties (Yankovich et al. 2019). The DOS1 method was applied to correct atmospheric

106 disturbances. Resultant surface reflectance and brightness temperature (K) bands were
107 then used in the further calculation of LST (°C), and LULC retrieval.

108 *2.3.2 LST retrieval*

109 LST was derived from the brightness temperature of band 06 and 10 of Landsat TM and
110 TIRS respectively. Corrected near-infrared (NIR) and Red bands were used to calculate
111 NDVI. It is calculated by dividing the differences between NIR and Red with their sum to
112 correct brightness temperature against land surface emissivity. The NDVI threshold
113 method was applied to estimate surface emissivity. The proportion of vegetation (Pv) was
114 determined using the following equation1 (Carlson and Ripley 1997).

$$Pv = \left[\frac{(NDVI - NDVIs)}{(NDVIv - NDVIs)}\right]^2 \quad (1)$$

115 Where, NDVIs and NDVIv is the value assigned for bare soil (0.2), and healthy
116 vegetation (0.5) respectively.

117 It is essential to obtain surface emissivity for accurate measurement of LST since it is a
118 proportionality factor that scales blackbody radiance (Planck's law) and predict radiance
119 (Jiménez-Muñoz et al. 2006). The emissivity was conditionally determined (Wang et al.
120 2015) from equation (2).

$$\varepsilon = \varepsilon_v P_v + \varepsilon_s(1-P_v) + C \quad (2)$$

121 Where, εv is vegetation emissivity, εs is soil emissivity and C represents the cavity effect
122 of the surface (C=0 for flat surfaces) was estimated using equation (3)

$$C=(1-\varepsilon_s)(1-P_v)F\,\varepsilon_v \quad (3)$$

123 Where, F is a shape factor, whose mean value is 0.55 assuming different geometrical
124 distributions (Sobrino et al. 2004) in the area.

125 For TIRS band 10, when the NDVI is less than 0, the emissivity value of 0.991 is
126 assigned considering pixels as water. For values between 0and 0.2, the emissivity value
127 of 0.966 is assigned considering pixels as soil. For values between 0.2 and 0.5, equation

(2) is applied to retrieve the emissivity considering pixels as mixtures of vegetation and soil. At last, when the NDVI value is greater than 0.5, the value 0.973 is assigned considering pixels to be covered with vegetation.

For TM band 06, simplified equation (4) is used to determine emissivity (Sobrino et al. 2004).

$$\varepsilon = 0.004Pv + 0.986 \quad (4)$$

Finally, the emissivity correction of LST was carried out using the following equation (5) (Avdan & Jovanovska 2016).

$$T_s = \frac{BT}{\left\{1+\left[\frac{\lambda \sigma BT}{hc}\right].ln\varepsilon\right\}} - 273.15 \quad (5)$$

Where, Ts is the LST (°C), BT is at-sensor brightness temperature (K), λ is the effective wavelength of the radiance, σ is Boltzmann constant (1.38 × 10−23 J/K), h is Planck's constant (6.626 × 10−34 Js), c is the velocity of light in a vacuum (2.998 × 10−8 m/sec) and ε is emissivity.

2.3.3 UTFVI calculation

Several indices of thermal comfort are available for assessing the UHI impacts on the quality of urban life (Ahmed 2018; Guha et al. 2018). UTFVI was calculated for quantitative evaluation of the impact of UHI using equation (6) and divided into six levels corresponding to ecological evaluation indices and UHI phenomenon intensity shown in Table 5 (Guha et al. 2018).

$$UTFVI = \frac{Ts - Tm}{Tm} \quad (6)$$

Where Ts and Tm are LST (°C) and mean LST (°C) respectively.

2.3.4 LULC classification

There have been many classification algorithms developed and implemented to classify images. Machine learning (ML) classifiers (e.g., random forest, support vector machine) is being popular for their high accuracy and robustness (Zhu & Woodcock 2014; Belgiu

and Drăguţ 2016). For this study, Random forest (RF) was used to LULC classification of 4 different years according to the classification scheme of Table 2. RF is a non-parametric ML algorithm, can handle high dimensional data (Gislason et al. 2006). It is an ensemble of decision trees which are trained on bootstrapped samples of original training datasets. For classification, each tree provides a class-label and the output is determined by the mostly voted class of the trees. In RF, two-third of the training samples are used to classify and another one-third is considered as out-of-bag (OOB) data. These OOB data are then used to produce a non-biased measurement of the error rate of classification (Breiman 2001).

3 Result

3.1 LST Trajectory

Before conducting any kind of application procedure, validation of extracted LST is essential with in situ observations or with another kind of satellite sensor. In this research, air temperature data were collected from different sources for the study area. Air temperature and LST of similar dates were compared and validated. The range of LST of the study area closely approximates with the air temperature of that area. The spatial extent and magnitude of LST have become more salient during 2020 from the past. Spatial distribution and descriptive statistics of LST of the corresponding year is represented in Table 3 and Fig. 2. A significant increase in the mean and maximum LST was followed between 2000 and 2020. Around 75% of the area had a temperature of over 18°C in 1990 and decreased to closely 50% in 2000. More than 75% area in 2020 was occupied by temperatures above 22°C (Table 3). It is apparent from the table that LST of the previous decade (1990-2000) was less deviated from the mean value which shows more variability in the recent decade (2010-2020). The lower central regions were relatively higher than the surroundings during 1990 and 2000. Peripheral areas have shown a decrease in LST from 1990 to 2000. In the years 2010 and 2020, some patches of extreme LST have been noticed in peripheral areas. Apart from that, a denser and high LST distribution can also be seen in the central zone (Fig. 2).

3.2 UHI identification

Validation of LULC classifications (1990 – 2020) involved collecting samples from high-resolution images of the closest dates available of Google Earth. Because of the unavailability of Google Earth's image during 1990 samples were collected from the corrected Landsat image of the year. Overall accuracy was achieved for all the classifications ranging from 94 to 96.2% with kappa accuracy ranging from 92 to 95%.

It can be seen from Fig. 3 that urban expansion took place in all directions. Noticeable expansion of urban areas has occurred northward and southeastward direction. A comparison of the LULC area and corresponding LST data between 1990 and 2020 is presented in Table 4. The developed surface dramatically increased throughout the period. The water surface showed a significant decline after 2000 followed by a moderate increase from 1990. Open soil decreased by 50% between 1990 and 2010 and significantly expanded afterwards.

Differences in mean LST of the developed surface to others are displayed in Fig. 4. The mean LST of the developed surface is higher than other classes supporting the existence of UHI. Open soil in 2010 and 2020 exhibits higher mean LST than developed areas and showed high variability than other classes from in both the years' Table 4. The reason behind this variability can be the contrasting nature of open soils in the study area. Open soil surfaces show an almost similar temperature to developed surfaces. In our study area, identified patches of open soil in Fig. 5 gives a close look to the corresponding surface in high resolution of Google Earth imagery. These surfaces are cleared bare soils for development purposes. These soils are drier than other barren surfaces of the study area which are mostly low lying lands.

3.3 UHI evaluation

UTFVI classification and relevant statistics are shown in Fig. 6 and Table 5 for comparative evaluation of the UHI impact over decades. Most of the regions were occupied with the strongest UHI (>0.020) and none UHI (<0). Strongest UHI spread spatially over time in upper eastern and southern regions (Fig. 6). Strongest UHI experienced in the study area showed a steady increase until 2010. In 2020, the strongest

UHI decreased from the previous year and showed the presence of strong and stronger classes of the UHI phenomenon.

According to the Ecological Evaluation Index (EEI), conditions ranging from bad to worst considerably increased, and above normal conditions showed a decline in contrast (Table 5). Ecological conditions ranging from bad to worst in the developed area showed progressive trends throughout the period whereas similar conditions in the non-developed area were regressive until 2010 and increased afterwards (Table 6). Figure 7 shows ecologically threatened developed surfaces in red color.

4 Discussion

The findings of the study show that the total environmental scenario of Dhaka was degraded in the developed area from 1990 to 2020 due to urban expansion as well as UHI intensification. Below normal ecological conditions showed considerable increase throughout the period, albeit the city central zone experiencing low UHI effect and having a normal ecological condition in 2020 (Fig. 6). There has not been an increase of vegetated or water surface in that zone to reduce the temperature and the rooftop garden is not extensively used (Farhana et al. 2019) which can mitigate the UHI effect. Therefore, the possible reason could be extreme heated open soils in surrounding patches shown in Fig. 6 influencing the LST normalization. Similar to Raja (2012), some open soil patches in adjacent urban areas show the highest LST in the years 2010 and 2020. These are the cleared or filled sites for new urban extensions (Fig. 5).

Highly centralized movement of people, along with an increase in urban population by birth increases pressure in cities. Dhaka receives 300,000 to 400,000 migrants annually for economic opportunities and other urban facilities (Lata 2017). This human pressure is the determinant of city expansion, both vertically and horizontally. Besides, the increasing concentration of the population in a particular region adversely affects the exploitation of the natural resources of the region (Rashid 2020). In response to its growth, the city is opening up new opportunities and facilities. This vicious nature of city dynamics keeps urban temperatures rising more frequently than the surrounding counterpart and constantly entraps city dwellers inside the UHI bubble. It is evident from

this study as well as previous literature (Ahmed et al. 2013; Dewan & Corner 2014) that developed surfaces along open dry soils release higher LST than other surface types (Table 4). With the rising temperature, energy demand also increases for cooling the building's inside environment and puts pressure on the electricity grid during peak hours. Uses of air cooler, refrigerator, etc. contribute to greenhouse gas volume which ultimately warms the earth (Calm 2002) and creates discomfort for us. Industrial chemicals, gashes, and contaminants create several environmental problems by modifying natural substances, create human health nuisance, and hamper an imbalance in biodiversity. In developing countries, the share of emitting greenhouse gases from urban areas is increasing rapidly. It is threatening for the urban dwellers' health; particularly the poor urban dwellers are in vulnerable conditions due to the newly created health hazards imposed by modified urban climate and a brief consideration of climate change (Oke 1982; Toy and Yilmaz 2010). Besides, due to the increasing trend of UHI and the influence of climate change, urban areas are more prone to undergo environmental hazards than their rural counterparts (Fig. 2). An approximate estimation of urban population facing below normal ecological conditions is 595,862.73 (9.3%) in 1990 which increased to 4,201,172 (19.8%) in 2020 (Fig. 7). Heat-related mortality and illness also increase with the rising temperature (Wu et al. 2018). The sensitive population especially children and older people of the city are more vulnerable to heat-initiated diseases (McMichael et al. 2008). On the contrary, the less intense winter season decreases the rate of cold-induced death. But in urban areas, hot microclimate also damages the atmospheric layer and produces an increasing amount of photochemical smog (for example, ozone); thus health risks also increase. UHI also degrades the quality of water sources in different ways. One of the foremost reasons is the heat-generating wastages coming from industries and other urban sources. Runoff from urban areas is hotter than the adjacent countryside in the summer season while the temperature of the pavement is higher than the air temperature. Runoff with high-temperature causes damage to young plants on its way and affect the ecosystem of water bodies and wetlands. It is observed in association with Islam et al. (2010) that the water surfaces are declining. Thus thermal alteration of water surfaces is adding to the problems already being faced from the reduction of water occupied areas. Fish communities are much likely to change

in growth, abundance, community structure, and richness due to this warming (Jeppesen et al. 2010, Pörtner and Peck 2010). Pörtner and Peck (2010) discussed that thermal tolerance varies among species and their life stages as well which in turn affects ecosystem productivity.

The pressure on the ecosystems of the world is increasing due to the influential role of urban inhabitants. As a result, cities have significantly large ecological footprints. Urbanization also offers some ecological benefits, among them shared use of the resource, opportunities for reuse and recycling and economies of scale are primes. To make effective use of the urban ecosystem and produce most of the outcomes, it is necessary to achieve a sustainable means of obtaining ecosystem services. Hence, UHI mitigation practices need to be deployed as early as possible. Both nature-based solutions (i.e. rooftop gardening, green spaces) and technical solutions (i.e. white rooftop, solar panel on the roof) can be used to reduce the UHI effect. Residential areas can use rooftop gardening to reduce heat and create spaces by applying the floor area ratio (FAR) for more green cover (Mahtab-uz-Zaman et al. 2007). A newly built environment such as the Basundhara Residential Area which is facing the worst case of heat stress must consider these mitigating measures. The solar panel seems to be a viable solution for mitigating UHI and energy consumption in industrial and commercial areas to an extent (Masson 2014).

5 Conclusion

Extensive urbanization factored by rapid population growth and economic development impacting local climates in metropolitan areas. UHI is the boomerang effect of unplanned urban development. Transformation of big cities into UHI is considered as one of the most highlighted results of microclimate change. The purpose of the current study was to determine the impact of UHI on the ecosystem of Dhaka city. This study has shown that high UHI experienced area, as well as the worst ecological condition, is expanding considerably in the city especially over the developed surfaces. The findings of this study based on satellite remote sensing analysis generate valuable information regarding urban health from the UHI mapping which can be used as an important reference for planners,

stakeholders, policymakers to aid in the mitigation measures. Further research can be carried out to assess the viability of the different mitigating solution and analyze the thermal tolerance of the urban ecosystem components.

Acknowledgements

Authors are thankful to the Climatic Research Group (CRG), Department of Geography and Environmental Studies, University of Chittagong for providing different sorts of supports during the study.

References

Ahmed B, Kamruzzaman M, Zhu X, Rahman M, Choi K (2013) Simulating land cover changes and their impacts on land surface temperature in Dhaka, Bangladesh. Remote Sens 5(11):5969-5998 https://doi.org/10.3390/rs5115969

Ahmed S (2018) Assessment of urban heat islands and impact of climate change on socioeconomic over Suez Governorate using remote sensing and GIS techniques. Egypt J Remote Sens Space Sci 21(1):15-25 https://doi.org/10.1016/j.ejrs.2017.08.001

Arnfield AJ (2003) Two decades of urban climate research: a review of turbulence, exchanges of energy and water, and the urban heat island. Int J Climatol 23(1):1-26 https://doi.org/10.1002/joc.859

Avdan U, Jovanovska G (2016) Algorithm for automated mapping of land surface temperature using LANDSAT 8 satellite data. J Sens 2016:1-8 https://doi.org/10.1155/2016/1480307

Belgiu M, Drăguţ L (2016) Random forest in remote sensing: A review of applications and future directions. ISPRS J Photogramm Remote Sens 114:24-31 https://doi.org/10.1016/j.isprsjprs.2016.01.011

Bivand R, Keitt T, Rowlingson B (2018) Bindings for the "Geospatial" Data Abstraction Library [R Package Rgdal Version 0.8-13] https://CRAN.R-project.org/package=rgdal

Breiman L (2001) Random forests. Mach Learn 45(1):5-32 https://doi.org/10.1023/A:1010933404324

325 Calm JM (2002) Emissions and environmental impacts from air-conditioning and
326 refrigeration systems. Int J Refrig 25(3):293-305 https://doi.org/10.1016/S0140-
327 7007(01)00067-6
328 Carlson TN, Ripley DA (1997) On the relation between NDVI, fractional vegetation
329 cover, and leaf area index. Remote Sens Environ 62(3):241-252
330 https://doi.org/10.1016/S0034-4257(97)00104-1
331 Choudhury AM (2016). Climate of Bangladesh. MET Report, 08/2016 ISSN 2387-4201,
332 159.
333 Das MK, Karmakar S (2015) Urban Heat Island Assessment for a Tropical Urban Air-
334 Shed in Bangladesh. In: Proceedings of the 9th International Conference on Urban
335 Climate jointly with 12th Symposium on the Urban Environment , France.
336 Dewan A, Corner R (2014) Impact of land use and land cover changes on urban land
337 surface temperature. In: Dewan A, Corner R, eds. Dhaka Megacity. Springer
338 Netherlands, pp 219-238 https://doi.org/10.1007/978-94-007-6735-5
339 Farhana F, Islam N, Zubayer S, Ahmed NU (2019) Green Roof: An approach to repair
340 the climate of Dhaka city. In: Proceedings of the 55th ISOCARP World Planning
341 Congress.
342 Gislason PO, Benediktsson JA, Sveinsson JR (2006) Random Forests for land cover
343 classification. Pattern Recognit Lett 27(4):294-300
344 https://doi.org/10.1016/j.patrec.2005.08.011
345 Grimm NB, Faeth SH, Golubiewski NE, Redman CL, Wu J, Bai X, Briggs JM (2008)
346 Global change and the ecology of cities. Science 319(5864):756-760
347 https://doi.org/10.1126/science.1150195
348 Guha S, Govil H, Dey A, Gill N (2018) Analytical study of land surface temperature with
349 NDVI and NDBI using Landsat 8 OLI and TIRS data in Florence and Naples city,
350 Italy. Eur J Remote Sens 51(1):667-678
351 https://doi.org/10.1080/22797254.2018.1474494
352 He B-J, Zhu J, Zhao D-X, Gou Z-H, Qi J-D, Wang J (2019) Co-benefits approach:
353 Opportunities for implementing sponge city and urban heat island mitigation. Land
354 use policy 86:147-157 https://doi.org/10.1016/j.landusepol.2019.05.003
355 Hijmans RJ (2016) Geographic Data Analysis and Modeling [R Package Raster Version

2.5-8]. https://CRAN.R-project.org/package=raster

Isaya Ndossi M, Avdan U (2016) Application of open source coding technologies in the production of land surface temperature (LST) maps from Landsat: A PyQGIS plugin. Remote Sens 8(5):413 https://doi.org/10.3390/rs8050413

Islam MS, Rahman MR, Shahabuddin AKM, Ahmed R (2010) Changes in wetlands in Dhaka City: Trends and physico-environmental consequences. J Life Earth Sci 5:37-42 https://doi.org/10.1007/s10750-010-0171-5

Jeppesen E, Meerhoff M, Holmgren K, González-Bergonzoni I, Teixeira-de Mello F, Declerck SA, De Meester L, Søndergaard M, Lauridsen TL, Bjerring R, Conde-Porcuna JM (2010) Impacts of climate warming on lake fish community structure and potential effects on ecosystem function. Hydrobiologia 646(1):73-90 https://doi.org/10.1007/s10750-010-0171-5

Jiménez-Muñoz JC, Sobrino JA, Gillespie A, Sabol D, Gustafson WT (2006) Improved land surface emissivities over agricultural areas using ASTER NDVI. Remote Sens Environ 103(4):474-487 https://doi.org/10.1016/j.rse.2006.04.012

Kakon AN, Nobuo M (2009) The sky view factor effect on the microclimate of a city environment: A case study of Dhaka City. In: Proceedings of the 7th International Conference on Urban Climate, Yokohama, Japan (Vol. 29).

Kuhn M (2020) Classification and Regression Training [R Package Caret Version 6.0-86]. https://CRAN.R-project.org/package=caret

Lata LN (2017) Migration and Urban Livelihoods: A Translocal Perspective in Dhaka, Bangladesh. In: Conference Proceedings TASA 2017 Conference.

Li D, Bou-Zeid E, Oppenheimer M (2014) The effectiveness of cool and green roofs as urban heat island mitigation strategies. Environ Res Lett 9(5):055002 https://doi.org/10.1088/1748-9326/9/5/055002

Li Z-L, Si M, Leng P (2020) A review of remotely sensed surface urban heat islands from the fresh perspective of comparisons among different regions (invited review). Prog Electromagn Res C Pier C 102:31-46 http://dx.doi.org/10.2528/PIERC20020403

Li ZL, Tang BH, Wu H, Ren H, Yan G, Wan Z, Trigo IF, Sobrino JA (2013) Satellite-derived land surface temperature: Current status and perspectives. Remote Sens Environ 131:14-37 https://doi.org/10.1016/j.rse.2012.12.008

387 Mahtab-uz-Zaman QM, Mallick FH, Abdullah AQM, Ahmad J (2007) In Search of a
388 Habitable Urban Space-Built Ratio: A Case Study of Building and Planning
389 Regulation in Dhaka City. In Bay JH, Ong BL (eds) Tropical Sustainable
390 Architecture: Social and Environmental Dimensions. Architectural Press (Elsevier),
391 pp 125–147
392 Masson V, Bonhomme M, Salagnac JL, Briottet X, Lemonsu A (2014) Solar panels
393 reduce both global warming and urban heat island. Front Environ Sci 2:14
394 https://doi.org/10.3389/fenvs.2014.00014
395 McMichael AJ, Wilkinson P, Kovats RS, Pattenden S, Hajat S, Armstrong B,
396 Vajanapoom N, Niciu EM, Mahomed H, Kingkeow C, Kosnik M (2008) International
397 study of temperature, heat and urban mortality: the "ISOTHURM" project. Int J
398 Epidemiol 37(5):1121-1131 https://doi.org/10.1093/ije/dyn086
399 Mia B, Bhattacharya R, Woobaidullah ASM (2017) Correlation and Monitoring of Land
400 Surface Temperature, Urban Heat Island with Land use-land cover of Dhaka City
401 using Satellite imageries. Int J Res Geogr 3(4) http://dx.doi.org/10.20431/2454-
402 8685.0304002
403 Oke TR (1973) City size and the urban heat island. Atmos Environ 7(8):769-779
404 https://doi.org/10.1016/0004-6981(73)90140-6
405 Oke TR (1982) The energetic basis of the urban heat island. Q J R Meteorol Soc
406 108(455):1-24 https://doi.org/10.1002/qj.49710845502
407 O'Malley C, Piroozfar P, Farr ERP, Pomponi F (2015) Urban Heat Island (UHI)
408 mitigating strategies: A case-based comparative analysis. Sustain Cities Soc 19:222-
409 235 https://doi.org/10.1016/j.scs.2015.05.009
410 Pörtner HO, Peck MA (2010) Climate change effects on fishes and fisheries: towards a
411 cause-and-effect understanding. J Fish Biol 77(8):1745-1779
412 https://doi.org/10.1111/j.1095-8649.2010.02783.x
413 Rahman M, Avtar R, Yunus AP, Dou J, Misra P, Takeuchi W, Sahu N, Kumar P,
414 Johnson BA, Dasgupta R, Kharrazi A (2020) Monitoring effect of spatial growth on
415 land surface temperature in Dhaka. Remote Sens 12(7):1191
416 https://doi.org/10.3390/rs12071191
417 Raja DR (2012) Spatial analysis of land surface temperature in Dhaka metropolitan area.

418 J Bangladesh Inst. Plann 5:151-167
419 Rashid KJ, Hoque MA, Esha TA, Rahman MA, Paul A (2020) Spatiotemporal changes of
420 vegetation and land surface temperature in the refugee camps and its surrounding
421 areas of Bangladesh after the Rohingya influx from Myanmar. Environ Dev Sustain
422 2020:1-6 https://doi.org/10.1007/s10668-020-00733-x
423 Ryu YH, Baik JJ (2012) Quantitative analysis of factors contributing to urban heat island
424 intensity. J Appl Meteorol Climatol 51(5):842-854 https://doi.org/10.1175/JAMC-D-
425 11-098.1
426 Sahana M, Ahmed R, Sajjad H (2016) Analyzing land surface temperature distribution in
427 response to land use/land cover change using split window algorithm and spectral
428 radiance model in Sundarban Biosphere Reserve, India. Model Earth Syst Environ
429 2(2) https://doi.org/10.1007/s40808-016-0135-5
430 Seto KC, Güneralp B, Hutyra L (2012) R Global forecasts of urban expansion to 2030
431 and direct impacts on biodiversity and carbon pools. Proc Natl Acad Sci U S A
432 109(40):16083-16088 https://dx.doi.org/10.1073%2Fpnas.1211658109
433 Shahmohamadi P, Che-Ani AI, Maulud KNA, Tawil NM, Abdullah NAG (2011) The
434 impact of anthropogenic heat on formation of urban heat island and energy
435 consumption balance. Urban Stud Res 2011:1-9 https://doi.org/10.1155/2011/497524
436 Sobrino JA, Jiménez-Muñoz JC, Paolini L (2004) Land surface temperature retrieval
437 from LANDSAT TM 5. Remote Sens Environ 90(4):434-440
438 https://doi.org/10.1016/j.rse.2004.02.003
439 Stewart ID, Oke TR (2012) Local climate zones for urban temperature studies. Bull Am
440 Meteorol Soc 93(12):1879-1900 https://doi.org/10.1175/BAMS-D-11-00019.1
441 Tashnim J, Anwar MA (2016) Reasons and Remedies of Heat Island Phenomena for
442 Dhaka City: A Review. In: Proceedings of the 3rd International Conference on Civil
443 Engineering for Sustainable Development, pp 228-234
444 Toy S, Yilmaz S (2010) Evaluation of urban-rural bioclimatic comfort differences over a
445 ten-year period in the sample of Erzincan city reconstructed after a heavy earthquake.
446 Atmósfera 23(4):387–402
447 Trotter L, Dewan A, Robinson T (2017) Effects of rapid urbanisation on the urban
448 thermal environment between 1990 and 2011 in Dhaka Megacity, Bangladesh. AIMS

449 Environ Sci 4(1):145-167. https://doi.org/10.3934/environsci.2017.1.145
450 Tzavali A, Paravantis JP, Mihalakakou G, Fotiadi A, Stigka E (2015) Urban heat island
451 intensity: a literature review. Fresen Environ Bull 4(12b):4537–4554
452 Voogt JA, Oke TR (2003) Thermal remote sensing of urban climates. Remote Sens
453 Environ 86(3):370-384 https://doi.org/10.1016/S0034-4257(03)00079-8
454 Wang F, Qin Z, Song C, Tu L, Karnieli A, Zhao S (2015) An improved mono-window
455 algorithm for land surface temperature retrieval from Landsat 8 thermal infrared
456 sensor data. Remote Sens 7(4):4268-4289 https://doi.org/10.3390/rs70404268
457 Ward K, Lauf S, Kleinschmit B, Endlicher W (2016) Heat waves and urban heat islands
458 in Europe: A review of relevant drivers. Sci Tot Environ 569-570:527-539
459 https://doi.org/10.1016/j.scitotenv.2016.06.119
460 Watkins R, Palmer J, Kolokotroni M (2007) Increased temperature and intensification of
461 the urban heat island: Implications for human comfort and urban design. Built
462 Environ 33(1):85-96 https://www.jstor.org/stable/23289474
463 Wu J, Yunus M, Ali M, Escamilla V, Emch M (2018) Influences of heatwave, rainfall,
464 and tree cover on cholera in Bangladesh. Environ Int 120:304-311
465 https://dx.doi.org/10.1016%2Fj.envint.2018.08.012
466 Yankovich KS, Yankovich EP, Baranovskiy NV (2019) Classification of vegetation to
467 estimate forest fire danger using Landsat 8 images: Case study. Math Probl Eng
468 2019:1-14 https://doi.org/10.1155/2019/6296417
469 Yow DM (2007) Urban Heat Islands: Observations, Impacts, and Adaptation: Urban heat
470 islands: observations, impacts, and adaptation. Geogr compass 1(6):1227-1251
471 https://doi.org/10.1111/j.1749-8198.2007.00063.x
472 Zhou D, Xiao J, Bonafoni S, Berger C, Deilami K, Zhou Y, Frolking S, Yao R, Qiao Z;
473 Sobrino JA (2019) Satellite remote sensing of surface urban heat islands: Progress,
474 challenges, and perspectives. Remote Sens 11(1):48
475 https://doi.org/10.3390/rs11010048
476 Zhou D, Zhang L, Li D, Huang D, Zhu C (2016) Climate–vegetation control on the
477 diurnal and seasonal variations of surface urban heat islands in China. Environ Res
478 Lett 11(7):074009 https://doi.org/10.1088/1748-9326/11/7/074009
479 Zhou W, Qian Y, Li X, Li W, Han L (2014) Relationships between land cover and the

surface urban heat island: seasonal variability and effects of spatial and thematic resolution of land cover data on predicting land surface temperatures. Landsc Ecol 29(1):153-167 https://doi.org/10.1007/s10980-013-9950-5

Zhu Z, Woodcock CE (2014) Continuous change detection and classification of land cover using all available Landsat data. Remote Sens Environ 144:152-171 https://doi.org/10.1016/j.rse.2014.01.011

Figures

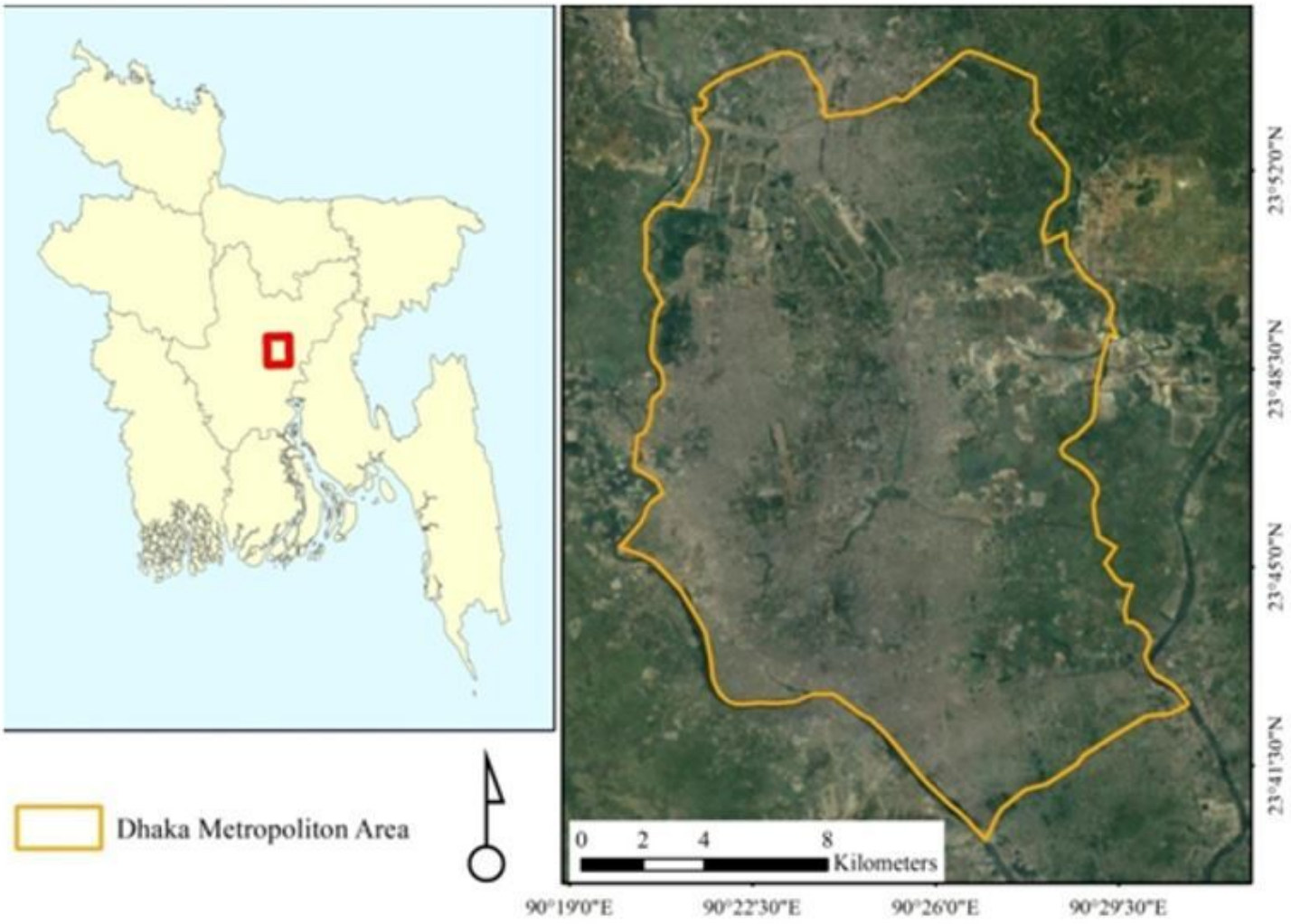

Figure 1

Study area showing administrative boundary of Dhaka Metropolitan Area (DMA)

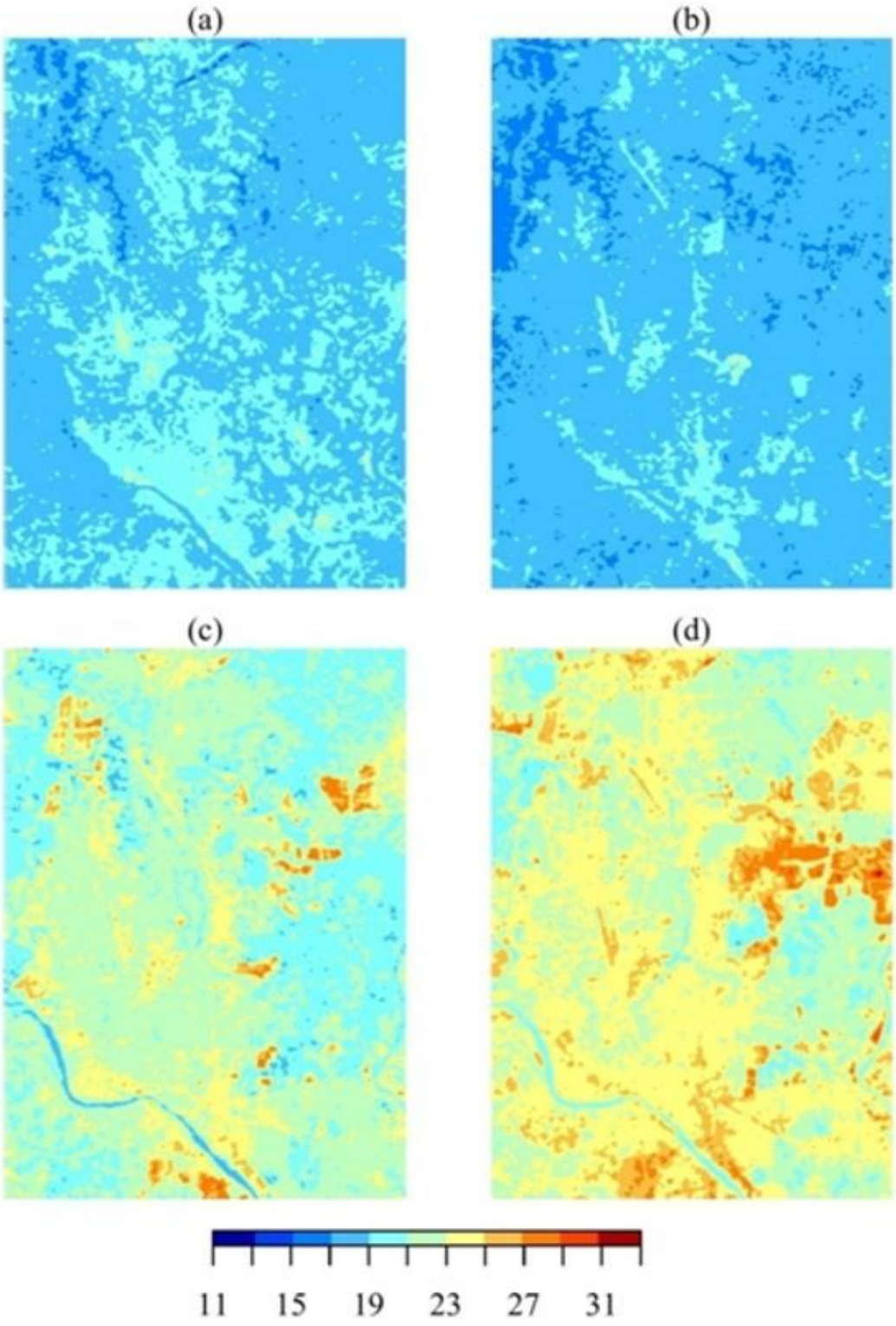

Figure 2

Spatio-temporal distribution of land surface temperature (LST) in the area where a, b, c, and d corresponds to the year 1990, 2000, 2010, and 2020 respectively

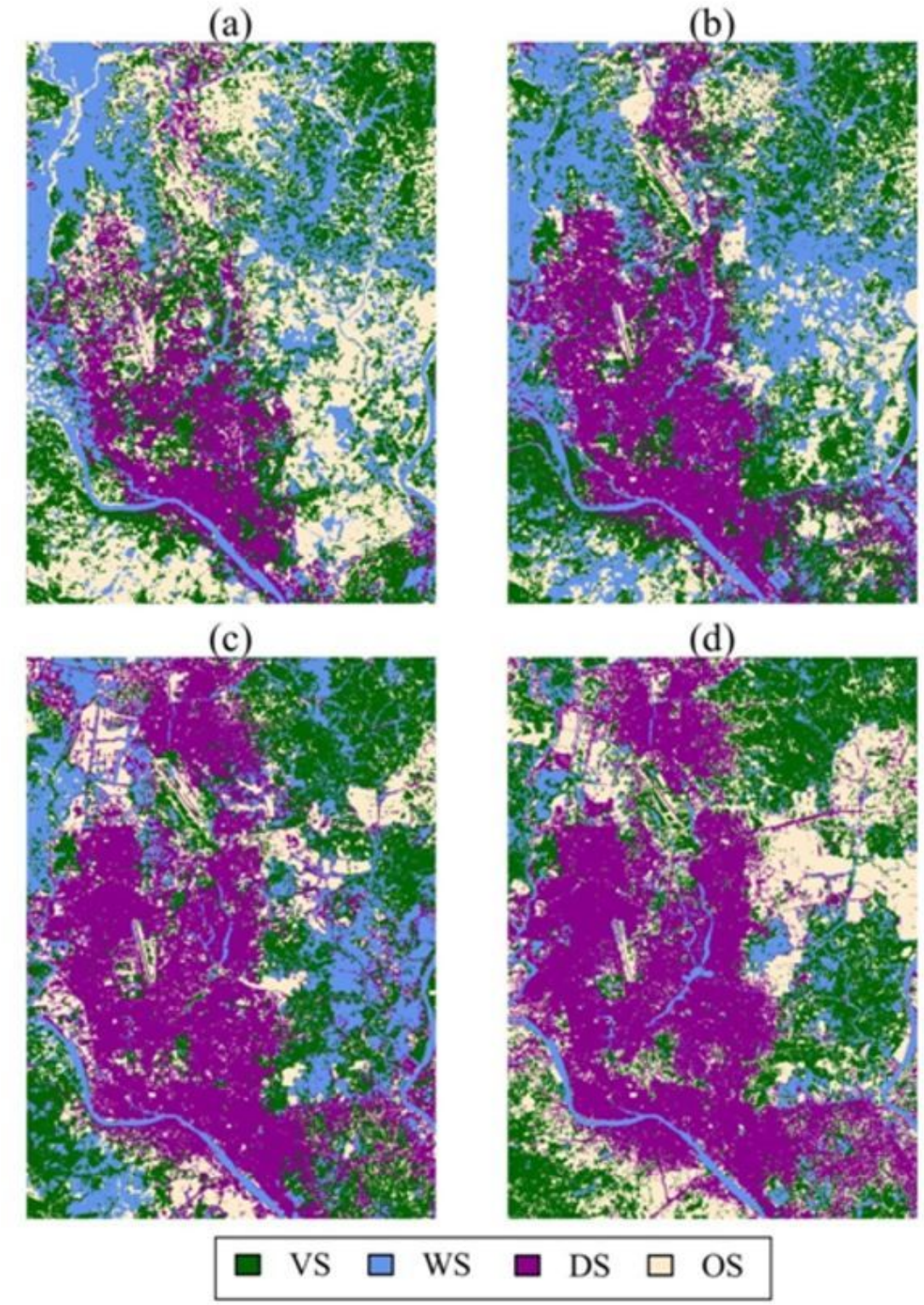

Figure 3

LULC classification maps of Dhaka city where a, b, c, and d corresponds to the year 1990, 2000, 2010, and 2020 respectively. Also VS, WS, DS, and OS are illustrated as vegetated surface, water surface, developed surface, and open soil accordingly.

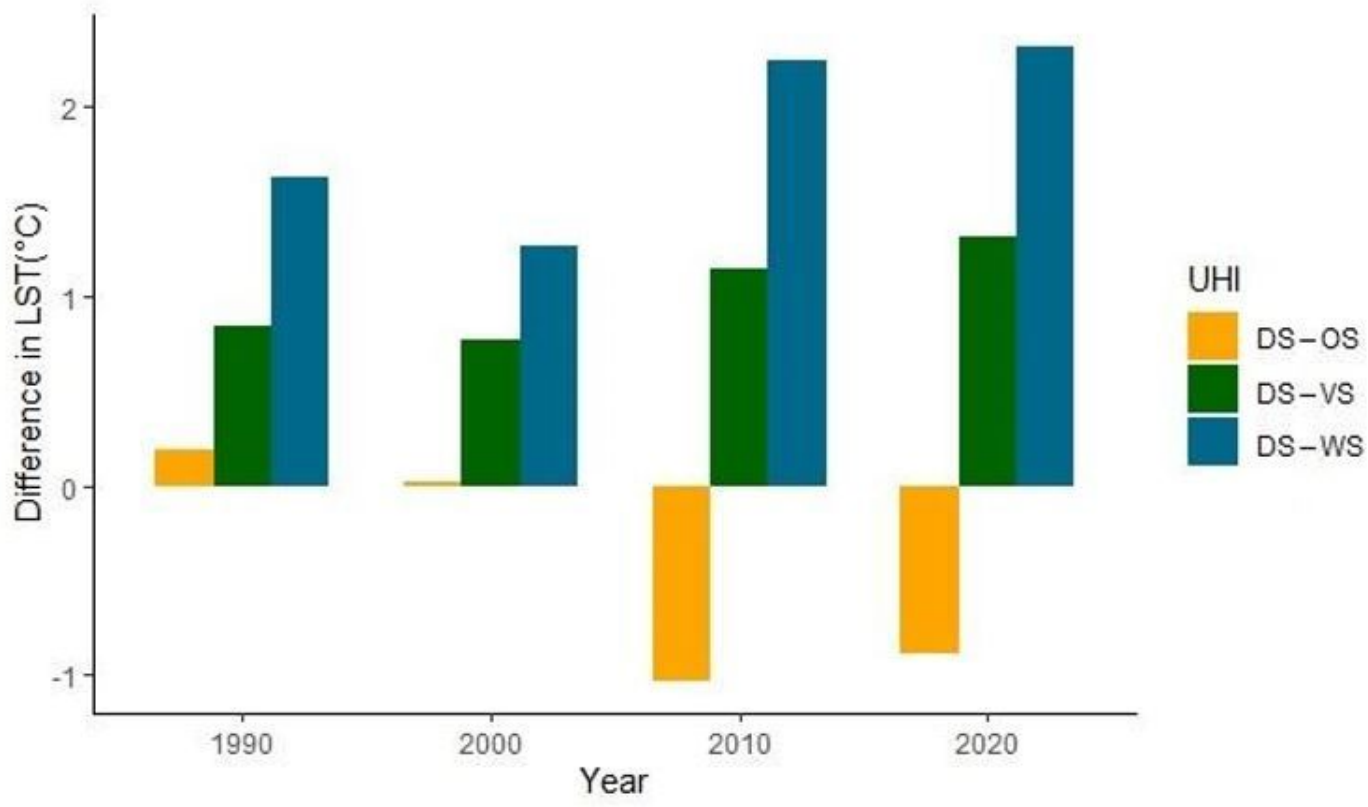

Figure 4

Difference of mean LST between developed surfaces (DS) and other LULC classes.

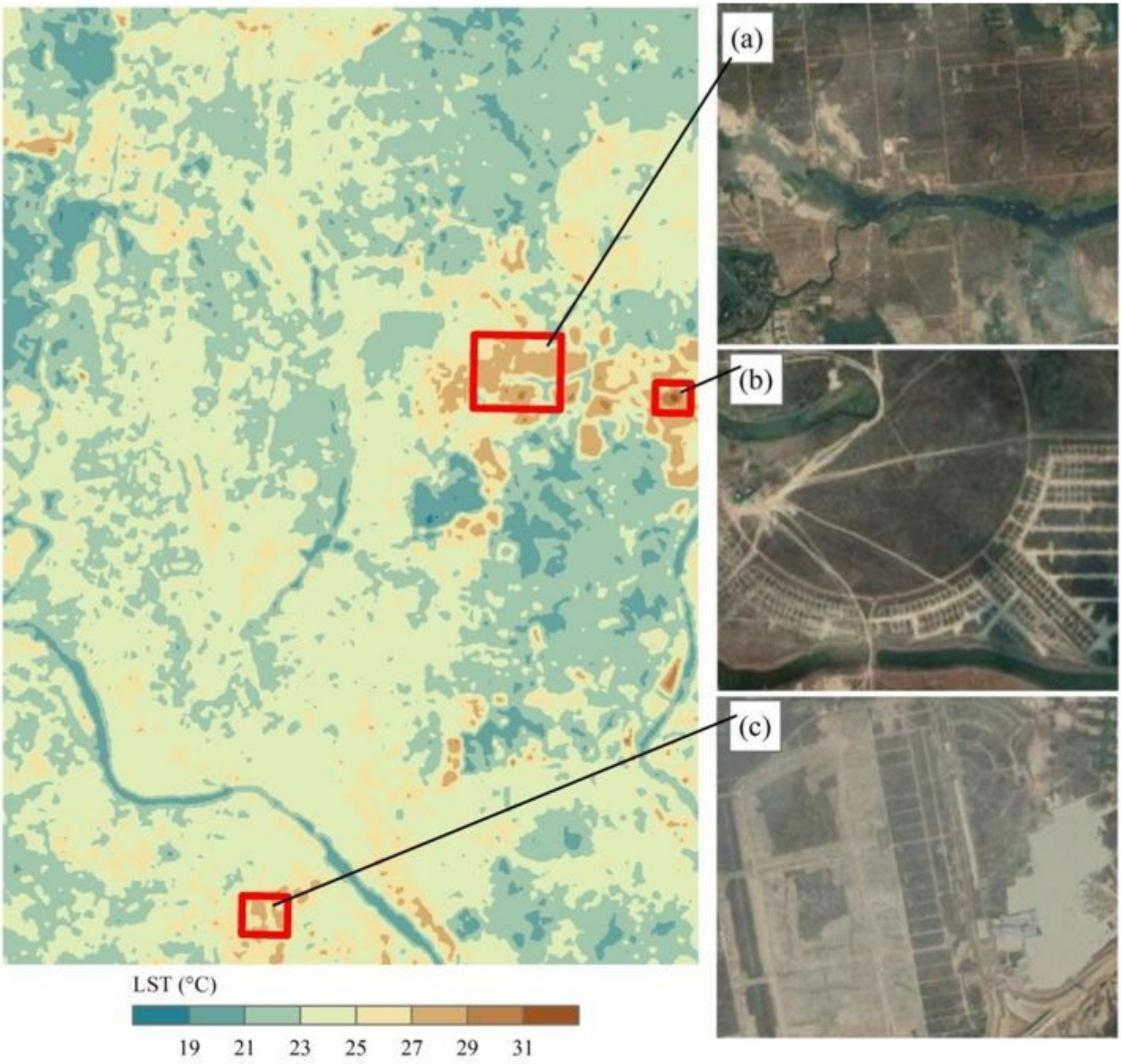

Figure 5

Patches of open soil showing extreme temperature.

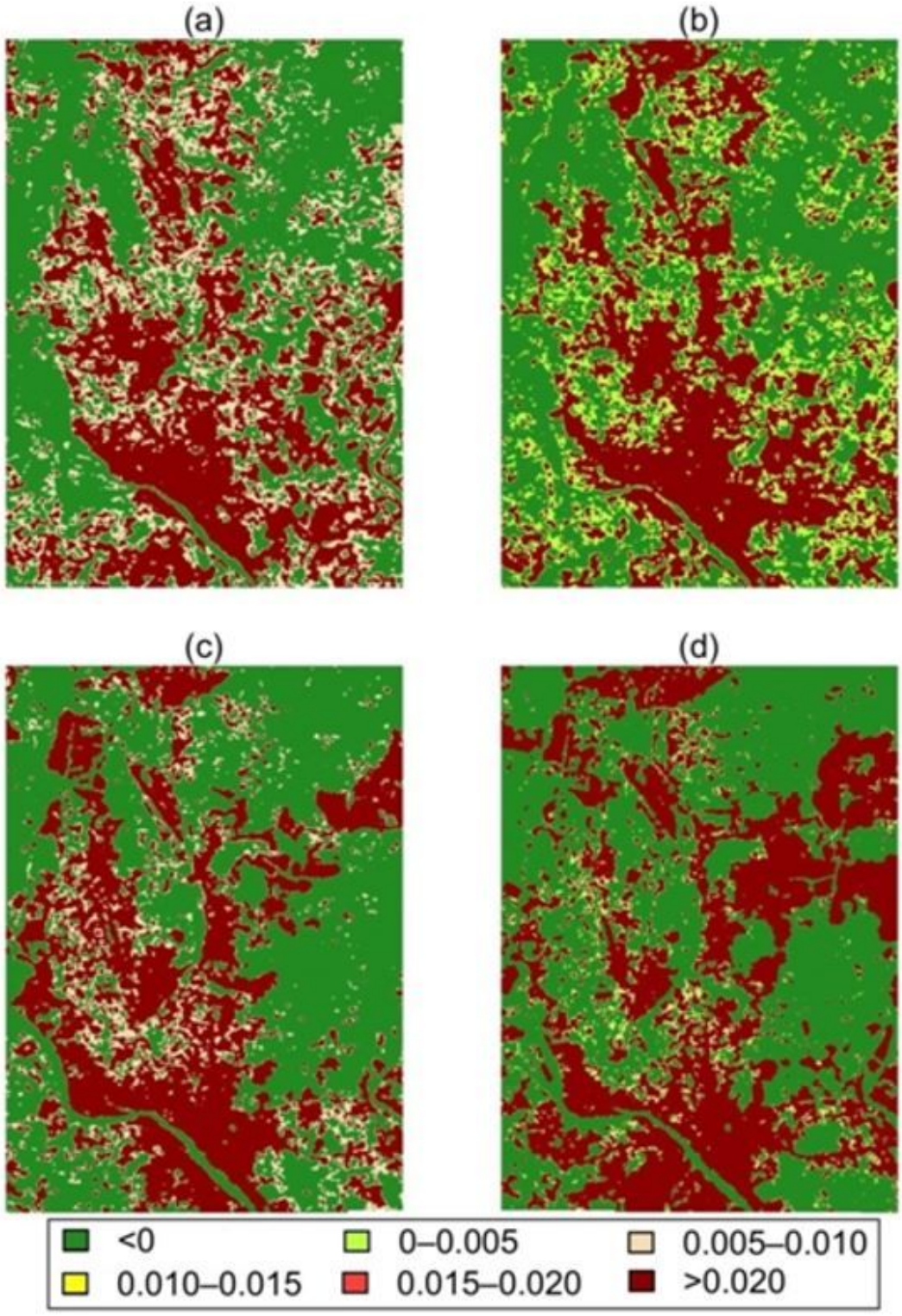

Figure 6

Urban thermal field variance index (UTFVI) classification into six classes according to the Table 5

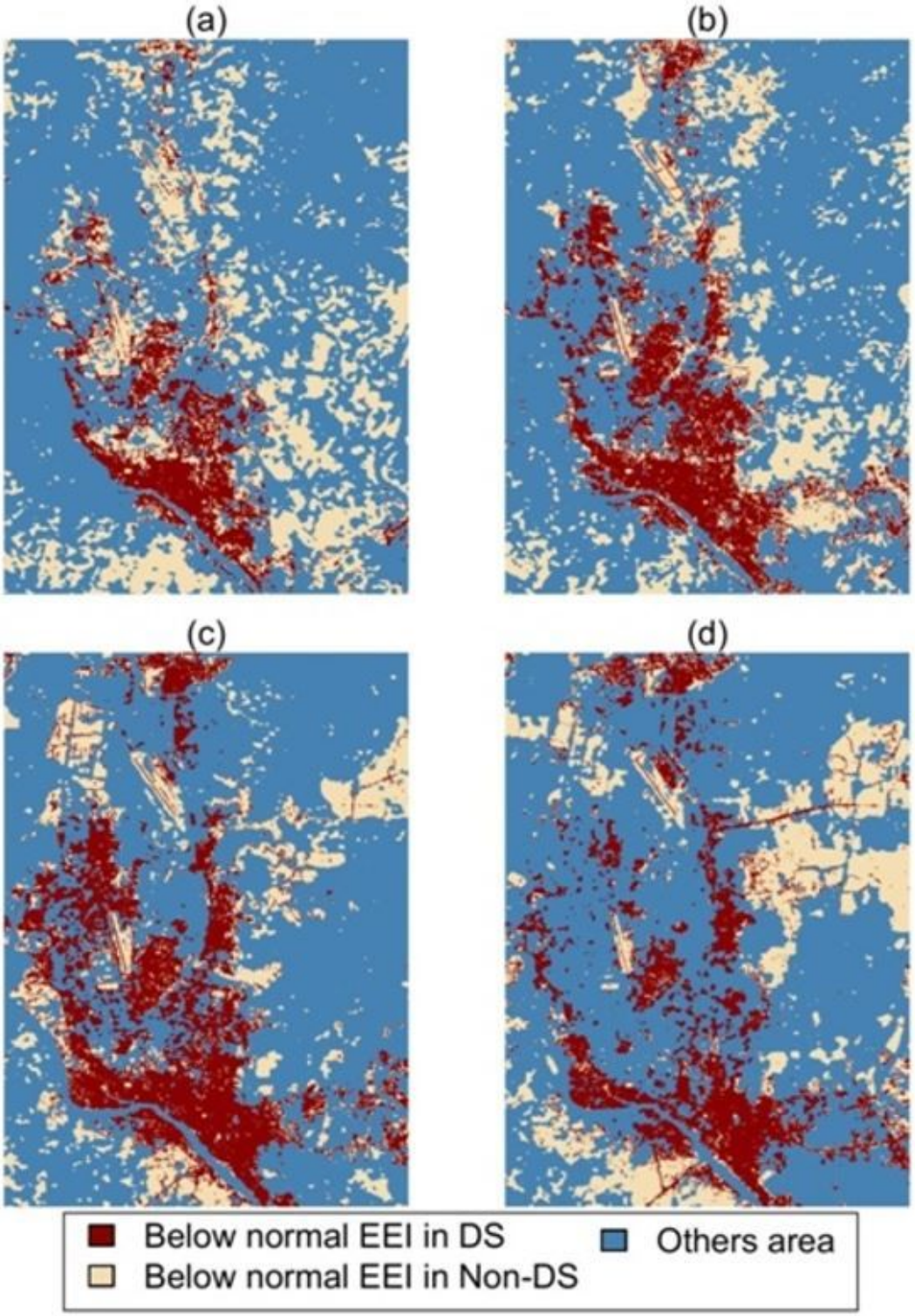

Figure 7

Comparison between LULC and UTFVI classification. 8